J. Chin. Inst. Chem. Engrs., Vol. 32, No. 1, 23-35, 2001

Evaluation of Multicomponent Mass and Energy Transfer through Vapor-Liquid Interfaces

Sergio D. Keegan, German D. Mazza and Guillermo F. Barreto*
Chemical Engineering Department, Faculty of Engineering,
National University of La Plata (UNLP), Calle 1 esq. 47,
(1900) La Plata - ARGENTINA
Research and Development Centre on Catalytic Processes (CINDECA)
CONICET - UNLP, Calle 47 No. 257; C. C. 59.
(1900) La Plata - ARGENTINA

Abstract — The solution of mass and heat transfer equations based on the Maxwell Stefan approach through vapor-liquid interfaces is analysed. The performance of the Newton method and two equation-tearing algorithms are compared. One of the equation-tearing algorithms is the method employed by Mori et al. (1996). The second one (META) is a modification presented in this contribution.

The behaviour of mass transfer and equilibrium relationships is undertaken as a first step in this study as this subset of equations defines the internal loop of both equation-tearing algorithms. From the analysis carried out a set of examples are selected (based on distillation and condensation problems) to evaluate the numerical procedures.

Mori et al. (1996) algorithm either fails to converge or it does making many iterations when mass transfer coefficients in both phases are of the same order. Instead, the Newton method and META do not show instances of divergence. The results found in this contribution show a significant saving in CPU time when using the META instead of the Newton method. Recalling the fact that the evaluation of interfacial fluxes will be one of the crucial building blocks in simulating liquid-vapor contacting devices with fully rated models, the META offers an appropriate alternative.

Key Words: Multicompoment Mass and Heat Transfer, Maxwell-Stefan Approach, Numerical Solution, Equation-Tearing Algorithms, Distillation and Condensation Problems

INTRODUCTION

There has been in the last decade an increasing interest in the use of rate based models for simulating processes involving multicomponent mass transfer. Rate based models avoid the use of efficiencies for correcting the results from equilibrium models, as has been done traditionally for separation processes. Also, more precise simulations can be obtained provided that transport properties, such as heat and mass transfer coefficients, are precisely evaluated (Taylor and Krishna, 1993).

An additional incentive for employing rate based models is the appearance of commercial processes employing reactive distillation for synthesis of fuel ethers such as MTBE or TAME (e. g. Paludetto et al., 1992), in particular, and the general trend to find more efficient reaction systems involving simultaneous separation and reaction functions (Ondry et al., 1996). Chemical reactions can keep liquid and vapor phases apart from phase equilibrium, particularly when the reactions take place at a rate at least comparable to that of mass transfer. It is thus likely that the significance of rate based models will be incremented in reactive distillation.

In most recent works mass transfer through the vapor-liquid interface is modelled by means of expressions based on Maxwell-Stefan constitutive equations coupled with a consistent energy balance (Taylor and Krishna, 1993; Sivasuvramanian, et al., 1987). These expressions should be solved along with the overall material and energy balances at each stage or position in the system.

Assuming that the state variables in the bulk of the phases are defined (in a given stage or section of a column), the non-linear heat and mass transfer equations should be solved iteratively to obtain the fluxes. The equations can be solved simultaneously by employing a Newton related method or some type of equation-tearing technique can be used by grouping equations and variables which are solved alternatively. A method of the latter type was recently suggested for packed column distillation by Mori et al. (1996), which in turn resembles the procedure described by Henley and Seader (1981). On the other hand, Taylor and Krishna (1993) in their monograph and more recently Taylor and Lucia (1995) suggested the use of Newton method.

The main objective of this contribution is to carry out a comparative analysis between Newton and e-

* To whom all correspondence should be addressed to: CINDECA-Calle 47 No. 257; C. C. 59, (1900) La Plata - ARGENTINA

quation-tearing approaches, with regards to computational implementation and computing times, when they are applied to solve the Maxwell-Stefan equations coupled to interfacial equilibrium relations and employing the interfacial energy balance as the bootstrap condition (Taylor and Krishna, 1993). The basic motivation behinds this purpose was to select a procedure with safe convergence towards the solution for a wide kind of problems (separation processes, multicomponent condensation and two-fluid phase reactors) and from wide ranges of initialization variables.

For the case of the so-called equation-tearing technique, two related algorithms will be tried here: the algorithm proposed by Mori et al (1996) and a modification presented in this contribution.

Mori et al. (1996) procedure employs 3 loops. No solution of linear systems nor derivative evaluation is needed for this algorithm.

The modification of Mori et al.'s algorithm presented here iterates on two variables in a nested fashion (two loops). Derivatives are not needed either, but linear systems of dimension $(p-1)$ should be solved (p is the number of components in the mixture).

Newton method, as presented in Taylor and Krishna (1993), iterates simultaneously on $3p+1$ variables (molar fractions at both sides of the interface, interfacial temperature and molar fluxes). Derivatives are needed and solution of linear systems of dimension $3p+1$ is involved.

This brief description of the numerical methods intends to show that they arrange the equations and variables in a very different way. With the aim of comparing their main features, mainly computational efficiency, different cases have been analysed. These cases are distinguished according to the type of solutions admitted by the Maxwell-Stefan equations coupled to the equilibrium conditions at the interface, regardless of the bootstrap condition (the interfacial energy balance). Although the different cases are derived from examples originally given for distillation and multicomponent condensation, they are expected to represent other processes involving multicomponent mass transfer. The paper will be organised as follows. First, a brief description of the equation modelling multicomponent mass transfer is given. The different cases, on the basis of the mass transfer equations alone, are presented next, followed by a discussion of the main features of the solutions reached when the heat transfer equation is employed to close the problem. The algorithms for solving the equations are presented and, finally, the performance of the algorithms when applied to the different cases is analysed.

MULTICOMPONENT MASS AND HEAT TRANSFER EXPRESSIONS

The Maxwell-Stefan approach is employed to evaluate multicomponent molar fluxes on each side of the vapor-liquid interface at steady state conditions. As it is well justified by Taylor and Krishna (1993), the integration of the Maxwell-Stefan original equations can be carried out in a rather simple way, on the basis of the following assumptions:

- Film theory is employed at both sides.
- No chemical reaction takes place inside the films.
- Average values between interfacial and bulk molar fractions are employed to evaluate the composition dependence of the matrix of inverse binary diffusion coefficients (linearized theory, as described in section 8.4 of Taylor and Krishna, 1993). It is important to point out that Taylor and Krishna (1993) have extensively checked the results from this approximation on a large amount of problems.
- The ratio between binary diffusion coefficients and the film depth are replaced by low-flux mass transfer coefficients for the binary $i-j$ pair, κ_{ij}.
- The matrix of thermodynamic factors Γ_{ij} is evaluated at average values between interfacial and bulk temperature and molar fractions.

With these assumptions, the vectors of $(p-1)$ molar fluxes N_i (positive for vaporization) can be expressed for each phase as:

$$\underline{N} = N_T \underline{x}^b + N_T(\exp[\Psi_L] - [I])^{-1}(\underline{x}^b - \underline{x}^I) \quad (1)$$

$$\underline{N} = N_T \underline{y}^I + N_T(\exp[\Psi_V] - [I])^{-1}(\underline{y}^I - \underline{y}^b) \quad (2)$$

where:

$$[\Psi_L] = N_T[\Gamma_L]^{-1}[R_L]; [\Psi_V] = N_T[\Gamma_V]^{-1}[R_V]$$

For each phase,

$$R_{ii} = \frac{z_i}{\kappa_{ip}} + \sum_{k=1\neq i}^{p} \frac{z_k}{\kappa_{ik}}; R_{ij} = -z_i\left[\frac{1}{\kappa_{ij}} - \frac{1}{\kappa_{ip}}\right] \ (i \neq j), for \ i,j = 1,\cdots,p-1$$

$$\Gamma_{ij} = \delta_{ij} + z_i \left.\frac{\partial ln\gamma_i}{\partial z_j}\right|_{T,P,\Sigma}; \delta_{ii} = 1; \delta_{ij} = 0 (i \neq j), for \ i,j = 1,\cdots,p-1$$

where z_i stands for the molar fraction either in the liquid or vapor phase.

Low flux binary mass transfer coefficients κ_{ij} employed here are defined on the basis of molar fractions as driving forces (instead of molar concentrations).

The $p-$th molar flux is evaluated as $N_p = N_T - \sum_{i=1}^{p-1} N_i$.

The set of expressions is completed with the thermodynamic equilibrium conditions at the interface,

$$y_i^I = K_i^I x_i^I; \ i = 1,\cdots,p \quad (3)$$

and

$$\sum_{i=1}^{p} x_i^I = 1 \quad (4a)$$

$$\sum_{i=1}^{p} y_i^I = 1 \tag{4b}$$

where K_i^I is the equilibrium constant evaluated at interfacial conditions.

Energy balances on both sides of the interface are written under similar assumptions as for mass balances and considering that molar heat capacities remain constant along each film. The following expression arises for heat transfer through the interface

$$T_I(h_L^* + h_V^*) + \sum_{i=1}^{p} N_i \Delta H_i^{vap}(T_I) = T_L h_L^* + T_V h_V^* \tag{5}$$

where

$$h_V^* = \frac{h_V \Phi_V}{\exp\Phi_V - 1};\ \Phi_V = \sum_{i=1}^{p} \frac{N_i c_{p,i}^V}{h_V}$$

$$h_L^* = \frac{h_L \Phi_L}{1 - \exp(-\Phi_L)};\ \Phi_L = \sum_{i=1}^{p} \frac{N_i c_{p,i}^L}{h_L}$$

In most practical applications, the liquid side heat transfer coefficient is high enough to reduce $h_L^* = h_L$.

In condensation processes, it is usually valid to ignore subcooling of the condensate. Under this assumption, Eq. (5) can be used if h_L^* is replaced by a global heat transfer coefficient h_0 accounting for heat transfer resistances across the condensate, the wall and the coolant side, and T_L is replaced by the local coolant temperature T_C.

Once the composition and temperature in the bulk of both phases are specified, along with the fluid-dynamics conditions defining the transport coefficients, Eqs. (1) to (5) allow the evaluation of the interfacial condition (x_i^I, y_i^I, T_I) and the fluxes N_i.

THE BEHAVIOUR OF MASS TRANSFER EQUATIONS

A given physical system is considered here to be defined once the identity of components, composition and temperatures in the bulk of the phases and binary mass transfer coefficients are specified. Once the physical system is defined, the set of mass transfer equations and equilibrium relations (1) to (4) needs only one additional constraint to be solved. This constraint is called bootstrap and, as stated before, we deal in this paper with the heat transfer equation taken as such constraint.

The distinguishing features of a given physical system are mainly cast in the system of Eqs. (1) to (4) rather than in the heat transfer equation. Hence, the type of solution arisen from Eqs. (1) to (4) will be analysed in this section regardless of the bootstrap condition.

The relationship between interfacial temperature T_I and the total molar flux N_T (curve T_I, N_T) will be used to characterise the type of solutions admitted by a given physical system.

Let rewrite the first $(p-1)$ equilibrium conditions (3) in the way

$$\underline{x}^I = [K^I]^{-1} \underline{y}^I \tag{6}$$

where $[K^I]$ is the diagonal matrix of $(p-1)$ equilibrium constants K_i^I,

By replacing $\underline{x}^I$ from Eq. (6) into Eq. (1), and equating the flux vector $\underline{N}$ from Eqs. (1) and (2), the following expression is obtained after collecting the terms in $\underline{y}^I$ and dividing by $(I - exp[\Psi_V])$:

$$([A] + [K^I]^{-1})\,\underline{y}^I = \exp[\Psi_L]\,\underline{x}^b + [A]\exp[-\Psi_V]\,\underline{y}^b \tag{7}$$

where:

$$[A] = (\exp[\Psi_L] - [I])([I] - \exp[-\Psi_V])^{-1} \tag{8}$$

Assuming that the value of N_T is given, the numerical solution of Eqs. (3), (4) and (7) allows the evaluation of $\underline{x}^I$, $\underline{y}^I$, and T_I, providing in this way the relation between T_I and N_T. After the solution is found, the individual fluxes N_i can be calculated directly from either Eqs. (1) or (2) (see the end part of Appendix B in Keegan et al.[1], 2000) for a discussion about which expression is better from a numerical point of view).

Extreme values of the global molar flux, $N_T \to \infty$ or $N_T \to (-\infty)$, may occur only when all components are soluble in both phases, which means that all individual K_i, $i = 1, \cdots, p$, are finite non-zero values. Assuming this condition, convective transport dominates in both films as $N_T \to \infty$ or $N_T \to -\infty$. For the specific case $N_T \to \infty$, $\exp[\Psi_L] \to \infty$ and $\exp[-\Psi_V] \to 0$ from the definitions of $[\Psi_V]$ and $[\Psi_L]$. Replacing these limiting values in Eqs. (7) and (8)

$$N_T \to \infty \quad (\underline{y}^I = \underline{x}^b) \tag{9a}$$

Besides, from Eq. (1):

$$N_i = x_i^b N_T \tag{9b}$$

Following a similar reasoning for $N_T \to -\infty$, we obtain

$$N_T \to -\infty : (x^I = y^b) \tag{10a}$$

$$N_i = y_i^b N_T \tag{10b}$$

The interfacial temperature T_I satisfying Eqs. (3) and (9a) is the dew point temperature of a vapor mixture having the bulk liquid composition, T_D^L. Similarly, the value of T_I satisfying Eqs. (3) and (9b) is the bubble point temperature for a liquid mixture having

(1) A copy of Keegan et al. (2000) can be requested to the corresponding author.

the bulk vapor composition, T_B^V.

We can expect that feasible values of T_I corresponding to $-\infty < N_T < \infty$ span monotonously from T_B^V to T_D^L. This is not always true, as can be checked by considering the solution for very small global fluxes, $N_T \to 0$. From Eqs. (7) and (8) with $\exp[\Psi_V] \to (1+\Psi_V)$ and $\exp[\Psi_L] \to (I+\Psi_L)$,

$$(N_T \to 0)([A]+[K^I]^{-1})y^I = x^b + [A]y^b \quad (11)$$

$$(N_T \to 0)[A] = [\Gamma_L]^{-1}[R_L][R_V]^{-1}[\Gamma_V] \quad (12)$$

If we assume that the mass transfer resistance in the vapor film is much larger than in the liquid film, a nearly uniform composition profile will hold on the liquid side. This can be established by requiring that the diagonal terms of matrix [A] defined in Eq. (12), verify,

$$A_{ii} << 1 \quad (13)$$

and

$$A_{ii} << 1/K_i^I \quad (14)$$

From Eq. (11), $\underline{x}^I \approx \underline{x}^b$. Therefore, the equilibrium at the interface will correspond, approximately, to the bubble point temperature of the liquid phase at the operating pressure, $T_I \approx T_B$. It should be stressed that for this conclusion to be valid is necessary that Eq. (14) holds for all the p components when they are alternatively included in the group of $(p-1)$ mass transfer equations. In the presence of a "permanent" gas in the vapor phase (K_i extremely large), Eq. (14) will not hold for this component.

Recalling that always $T_B \leq T_D^L$, we can distinguish two cases when Eqs. (13) and (14) hold:

A) If $T_B > T_B^V$, T_B falls within the range (T_B^V, T_D^L), a monotonous trend can be expected for T_I.

B) If $T_B < T_B^V$, T_B falls outside the range (T_B^V, T_D^L), a minimum value of $T_I \approx T_B$ should be expected.

Examples of cases A and B are given in Figs. 1 and 2 for a four-component mixture of acetone (1), methanol (2), 2-propanol (3) and water (4) at 101 kPa. Binary mass transfer coefficients were taken from Example 12.3.3 of Taylor and Krishna (1993), corresponding to a distillation column with structured packing (Table 1). The vapor was considered to behave as an ideal gas ($[\Gamma_V]=[I]$) and the thermodynamic factors for the liquid phase were evaluated according to the NRTL model. $(\kappa_{ij}^V)_{av}$ employed as a reference value in Figs. 1 and 2 is the average value in the vapor phase, which from Table 1 $(\kappa_{ij}^V)_{av} = 5.624\ 10^{-4}$ kmol/(m^{2}s).

The difference between the systems corresponding to Figs. 1 and 2 is provided by the composition of the bulk phases.

Table 1. Binary mass transfer coefficients of components in mixtures of Figs. 1,2 and 4.

Binary mass transfer Coefficients κ_{ij} for pairs:	Vapor (Kmol/m^2 s)	Liquid (Kmol/m^2 s)
(1,2)	$0.4752\ 10^{-3}$	0.01143
(1,3)	$0.3520\ 10^{-3}$	0.01056
(1,4)	$0.6336\ 10^{-3}$	0.01195
(2,3)	$0.4642\ 10^{-3}$	0.01178
(2,4)	$0.8272\ 10^{-3}$	0.01385
(3,4)	$0.6204\ 10^{-3}$	0.01290

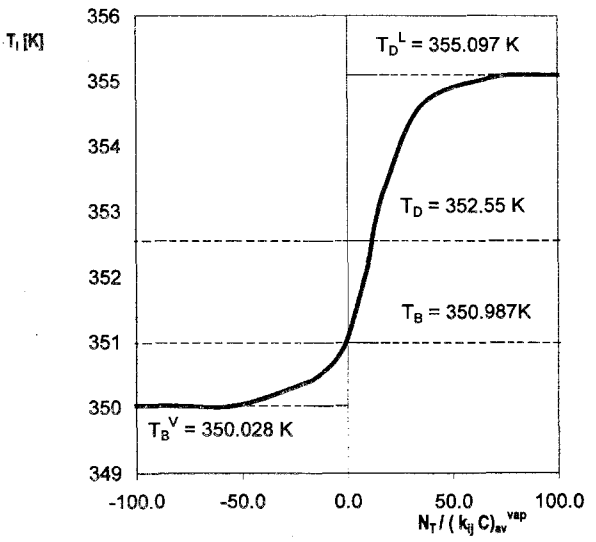

Fig. 1. Values of T_I vs. N_T for mixtures of acetone, methanol, 2-propanol and water with binary mass transfer coefficients given in Table 1.
$\underline{x}^b$ = (0.003159, 0.164701, 0.394518, 0.437623); $\underline{y}^b$ = (0.00411, 0.20935, 0.42352, 0.36302)
T_B = 350.987 K, T_D = 352.55 K, T_B^V = 350.028 K, T_D^L = 355.097 K.

Conditions (14) are well satisfied for these examples, as the resistance coefficients in the vapor phase are about 20 times those in the liquid phase and K_i values are of the order of unity. Case A) is illustrated in Fig. 1, where the interfacial temperature T_I is observed to increase monotonously with N_T. The liquid phase composition represents a less volatile mixture than the vapor phase mixture. Therefore, this case will be typical of most applications (vaporisation, condensation, distillation).

Two examples of Case B) are given in Fig. 2. They differ in the relative position of T_B^V and T_D^L, but the existence of minimum values of T_I around $N_T = 0$ is observed in both examples. The liquid phase composition corresponds in this case to a more volatile

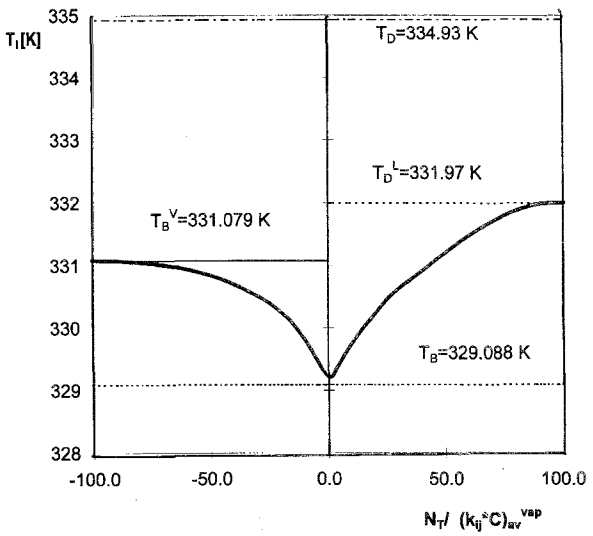

Fig. 2a. Values of T_I vs. N_T for mixtures of acetone, methanol, 2-propanol and water with binary mass transfer coefficients given in Table 1.
$\underline{x}^b = (0.6,\ 10^{-5},\ 0.3, 0.09999)$; $\underline{y}^b = (0.3,\ 10^{-5},\ 0.6,\ 0.09999)$; $T_B = 334.113$ K, $T_D = 348.19$ K, $T_B^V = 340.645$ K, $T_D^L = 339.765$ K.

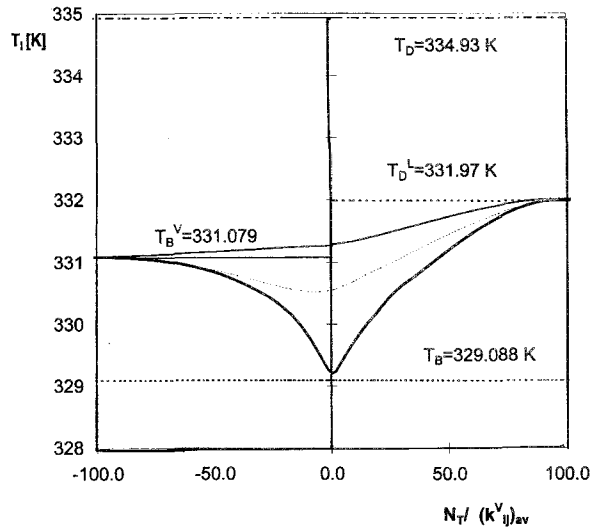

Fig. 2b. Values of T_I vs. N_T for mixtures of acetone, methanol, 2-propanol and water. Values of binary mass transfer coefficients are:
——— (Table 1); ····· (Table 2)
——— ($\kappa_{ij}^L = \kappa_{ij}^V$)
$x^b = (0.75,\ 0.16,\ 0.06,\ 0.03)$; $y^b = (0.7,\ 0.1,\ 0.1,\ 0.1)$;
$T_B = 329.09$ K, $T_D = 334.93$ K, $T_B^V = 331.079$ K, $T_D^L = 331.97$ K.

Table 2. Modified binary mass transfer coefficients used in Fig. 2b. The κ_{ij}^V values are about 40% smaller than κ_{ij}^L

Binary mass transfer Coefficients κ_{ij} for pairs:	Vapor (Kmol/m² s)	Liquid (Kmol/m²s)
(1,2)	$0.6817\ 10^{-2}$	0.01143
(1,3)	$0.6279\ 10^{-2}$	0.01056
(1,4)	$0.7176\ 10^{-2}$	0.01195
(2,3)	$0.7086\ 10^{-2}$	0.01178
(2,4)	$0.8252\ 10^{-2}$	0.01385
(3,4)	$0.7714\ 10^{-2}$	0.01290

mixture than the vapor phase mixture. Although Case B) is not common in practice, it is physically feasible and will be employed here to test the numerical procedures.

The presence of a maximum in the (T_I, N_T) is also possible if mass transfer is controlled by the liquid phase. In general, it can be concluded that a monotonous increasing curve (as that in Fig. 1) will hold if the range ($T_B - T_D$) is included in the range ($T_B^V - T_D^L$). Otherwise, an extreme can be present, depending on the ratio of binary mass transfer coefficients in both phases.

To evaluate the effect of the ratio of binary mass transfer coefficients in both phases, a new set of conditions can be obtained from the systems in Figs. 1 and 2 by increasing the values of κ_{ij}^V up to approach those of the liquid phase. The values defined in Table 2 correspond to κ_{ij}^V only 40% smaller than κ_{ij}^L. Practical cases showing this feature are likely, for example, in the rectifying section of distillation columns. On one hand, the effect produced by the coefficients defined in Table 2 on the (T_I, N_T) curves is to shift the values of T_I at $N_T = 0$ to an intermediate value between T_B and T_D. As a consequence, the minimum tends to disappear, as it is shown in Fig. 2b. The results achieved when $\kappa_{ij}^V = \kappa_{ij}^L$ are also plotted in Fig. 2b.

The final case considered here corresponds to a condensing mixture with the presence of a non-condensable component. The specific case was taken from the work of Mazzarotta and Sebastiani (1995), who analysed condensation of a water-ethanol mixture containing CO_2 in a vertical condenser. As CO_2 is considered a non-condensable component, the following equation can be applied for it:

$$K_{CO_2} \to \infty \tag{15a}$$

The so-called unmixed hypothesis which states

$$N_i = N_T x_i^b \tag{15b}$$

is employed for all condensable components in the liq-

Table 3. Condensation of a water-ethanol mixture in the presence of CO_2 in a vertical shell-and-tube condenser (1: CO_2; 2: ethanol; 3: H_2O).

Operating conditions	
Top	Bottom
$T_{coolant}$ = 313 K	$T_{coolant}$ = 303 K
T_V = 353 K	T_V = 333 K
Vapor mole fraction:	Vapor mole fraction:
y_1^b = 0.56	y_1^b = 0.782
y_2^b = 0.12	y_2^b = 0.110
y_3^b = 0.32	y_3^b = 0.108
Heat transfer coefficients [W/m^2 K]	
h_V = 146.33	h_V = 133.82
h_0 = 1397.79	h_0 = 413.22
Binary Mass Transfer Coefficients in the vapor phase κ_{ij}^V for pairs [Kmol/m^2 s]	
(1,2) = 2.6607 10^{-3}	(1,2) = 3.1404 10^{-3}
(1,3) = 1.6263 10^{-3}	(1,3) = 1.9195 10^{-3}
(2,3) = 1.9370 10^{-3}	(2,3) = 2.2864 10^{-3}

uid film. Equation (15*b*) replaces the assignment of bulk liquid composition. This hypothesis is physically sound for horizontal condenser or at the top of a vertical condenser, but it also produces good results for the full surface of vertical condensers, particularly when non-condensable components are present (Taylor and Krishna, 1993).

Equation (15*a*) leads to $N_{CO_2} = 0$. This condition prevents the system from the possibility of reaching large values of $(-N_T)$. Instead, N_T will approach a limiting value $N_{T,limit}$ as T^I decreases arbitrarily (corresponding to a vapor side interface built up entirely of the noncondensable component).

Recalling that N_T will be negative, it can be demonstrated that (15*b*) corresponds to the particular case of the general formulation (1) to (4) arisen when $(\kappa_{ij}^L/N_T) \rightarrow 0$, i.e. arbitrarily small liquid phase mass transfer coefficients (Eq. B-6 in Appendix B of Keegan et al., 2000).

Details about implementation of conditions (15*a*) and (15*b*) within the frame of the general formulation given by Eqs. (1) to (4) are provided in Appendix A of Keegan et al. (2000) along with an approximate expression to predict $N_{T,limit}$.

The relevant quantities employed at the top and bottom of the condenser are collected in Table 3. Heat transfer coefficients were calculated from relationships recommended by Mazzarota and Sebastiani (1995) in their work, and values of κ_{ij}^V were obtained from h_V by using the Chilton-Colburn's analogy (Bird et al., (1960). NRTL activity model was also employed in this example.

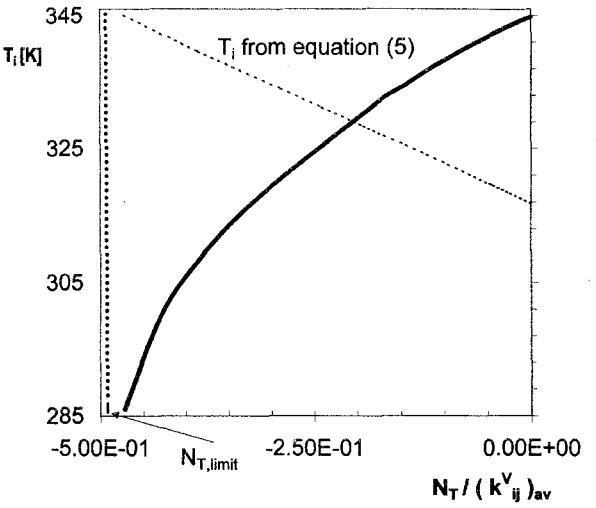

Fig. 3. Values of T_I vs. N_T and values of T_I from equation 5 for mixtures of water-ethanol in the presence of CO_2 at top conditions in the vertical shell-and-tube condenser given in Table 3.
(1: CO_2; 2: ethanol; 3: H_2O).

The $(T_I - N_T)$ curve for operating conditions at the top of the condenser is shown in Fig. 3. The dashed curve in Fig. 3 is explained in the next section.

SOLUTIONS EMPLOYING THE ENERGY BALANCE

The solution of the set of Eqs. (1) to (5) can be interpreted as the point of the curve (T_I, N_T) which simultaneously satisfies the heat transfer Eq. (5). From the known values N_i at each point of the mass transfer curve (T_I, N_T), a value of T_I can be calculated from Eq. (5). If this value coincides with the value of the curve (T_I, N_T), the solution is reached.

This procedure is depicted in Figs. 4a and 4b with a bulk liquid temperature two degrees below the bubble point, $T_L = (T_B - 2K)$, for the systems defined in Fig. 1 and Fig. 2b. Values of h_L were evaluated by assuming analogy between heat and mass transfer processes at low mass transfer rates. Two cases were considered: $[Sh/Nu] = [Sc/Pr]^{1/3}$ (Chilton-Colburn's analogy), and $[Sh/Nu] = [Sc/Pr]^{1/2}$ (Penetration model). The values so obtained are $h_L = 1.3\ 10^4\ W/(m^2\ K)$ and $h_L = 7.6\ 10^3$ W/(m^2 K), respectively. The Chilton-Colburn analogy was employed for the vapor heat transfer coefficient, resulting $h_V = 42 W/(m^2\ K)$.

The similar results for the top of the condenser considered in the previous section are shown in Fig. 3. It is recalled that in this case h_O replaces h_L and T_C

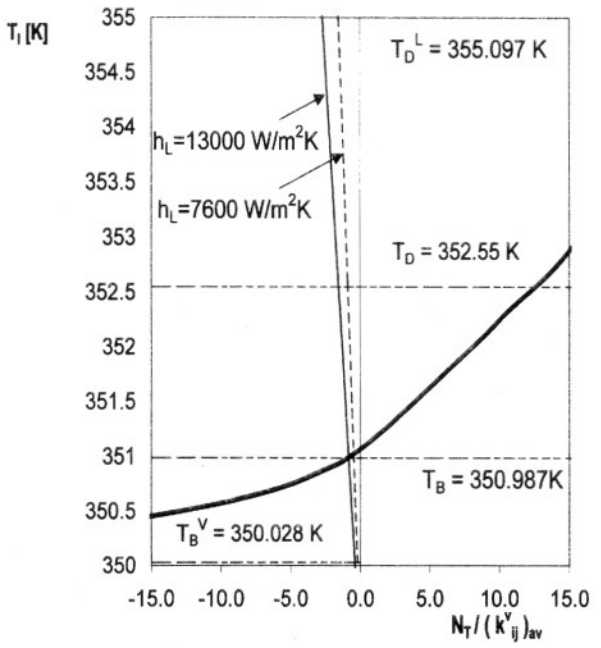

Fig. 4a. Values of T_I vs. N_T and values of T_I from Eq. (5) for mixtures and conditions corresponding to Fig. 1, with binary mass transfer coefficients given in Table-1. $T_L = 348.9$ K.

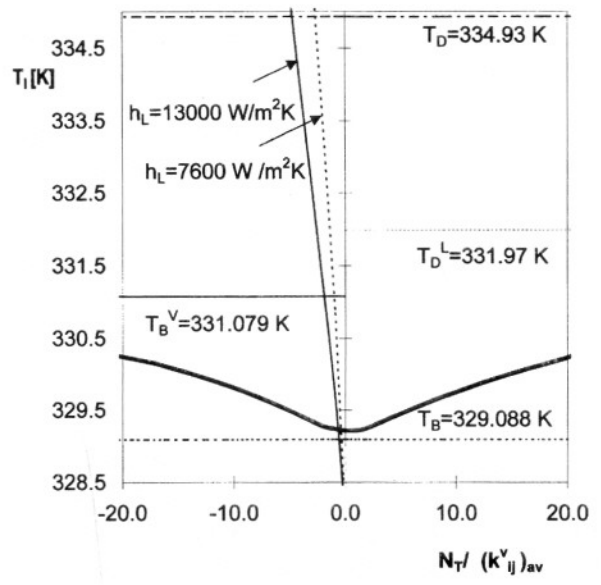

Fig. 4b. Values of T_I vs. N_T and values of T_I from equation (5) for mixtures and conditions corresponding to Fig. 2b, with binary mass transfer coefficients given in Table 1. $T_L = 328.0$ K.

replaces T_L in Eq. (5).

The solutions obtained in Figs. 4 correspond to points of the (T_I, N_T) curve close to $N_T = 0$. It can be easily shown that for systems showing values of

Table 4. Results for mixtures in Fig. 1 with $T_B - T_L = 1$℃ and $T_B - T_L = 0.1$℃

	Condition added to mass transfer equation to solve the system		
	$q_{latent} = 0$	Heat balance (eq. 5) $h_L = 13000$ W m^{-2}K^{-1} $T_B - T_L = 1$℃	Heat balance (eq. 5) $h_L = 13000$ W m^{-2}K^{-1} $T_B - T_L = 0.1$℃
T_I[K]	351.0671	351.0004	351.060
N_T [kmol/m^2 s]	$2.203\ 10^{-6}$	$-3.146\ 10^{-4}$	$-3.980\ 10^{-5}$
N_1[kmol/m^2 s]	$2.856\ 10^{-6}$	$7.973\ 10^{-7}$	$2.577\ 10^{-6}$
N_2	$3.331\ 10^{-5}$	$-3.941\ 10^{-5}$	$2.366\ 10^{-5}$
N_3	$6.162\ 10^{-6}$	$-1.281\ 10^{-4}$	$-1.154\ 10^{-5}$
N_4	$-4.012\ 10^{-5}$	$-1.478\ 10^{-4}$	$-5.434\ 10^{-5}$

Table 5. Comparison of the behaviour of numerical procedures for four components mixtures in Fig. 1. In all cases, $T_V = 360$ K.

			Computing time after 10000 executions of the program (in seconds)		
h_L [W/m^2 K]	T_L [K]	κ^L; κ^V from Table	Newton	Mori et al.	META
7600	348.987	1	23.5	53	18
	348.987	2	23	No convergence	24
	340.987	1	24.3	50.5	19
13000	348.987	1	24	53	22.5
	348.987	2	23	No convergence	14
	340.987	1	31	58	23

κ_{ij}^V smaller than those in Table 1, e. g. for processes with small ratios of vapor/liquid mass inputs, the solutions shift towards larger values of $[-N_T/(\kappa_{ij}^V)_{av}]$.

In the examples given in Figs. 4 the vapor side heat transfer coefficient h_V is about two orders of magnitude less than that in the liquid film. In the condenser, the ratio h_O/h_V is not so large, but h_V is still significantly smaller than h_O (see Table 3). Therefore, in Eq. (5) the term corresponding to the vapor phase is of secondary importance. This is a rather general conclusion for vapor-liquid contacting devices.

The driving force ($T_I - T_L$) or ($T_I - T_C$) then becomes paramount to determine the rate of latent heat exchange

$$q_{latent} = \sum_{i=1}^{p} \Delta H_i^{vap} N_i \tag{16}$$

In condensers, the value of T_C can be set according to the purpose of the process, by choosing the operating conditions of the coolant stream. In separation or mass transfer processes, there is not

an external sink (or source) such as the coolant stream, being the liquid stream the only mean to absorb q_{latent}. As a consequence, the difference $(T_I - T_L)$ becomes small for most part of the contacting device.

Based on this observation, Taylor and Krishna (1993) used the bootstrap condition $q_{latent} = 0$ instead of the heat transfer Eq. (5). Considering both alternatives, the results in Table IV summarized the values of N_T and individual fluxes N_i obtained from $q_{latent} = 0$ and those obtained with Eq. (5) for two values of $(T_B - T_L)$, 1 K and 0.1 K. Conditions defined in Fig. 1 were undertaken. Calculated values of the driving force $(T_I - T_L)$ from Eq. (5) are close to $(T_B - T_L)$, since, $T_I \approx T_B$ at the relatively small values resulting for N_T.

The value N_T for $q_{latent} = 0$ is almost nil, as the individual latent heats of vaporisation do not differ much among themselves. Very large differences between the absolute and relative values of the individual fluxes N_i calculated from $(T_B - T_L) = 1$ K and from $q_{latent} = 0$ can be appreciated in Table 4. Even for $(T_B - T_L) = 0.1$ K (condition where $T_B \approx T_L$) the differences persist, in particular for 2-propanol (component 3).

As commented on before, for a system showing similar values of κ_{ij} in both phases (as can be expected in the rectifying section of a distillation column) the values of T_I for small N_T will fall somewhere between T_B and T_D. Hence, as the bulk liquid temperature T_L can not rise above T_B, the driving force $(T_I - T_L)$ will become fairly large.

The significance of the previous discussion for simulating distillation columns is beyond the scope of this paper, but we believe worth noticing here that the results from employing the heat transfer Eq. (5) may depart significantly from those employing the condition $q_{latent} = 0$.

NUMERICAL PROCEDURES FOR THE SOLUTION OF MASS AND ENERGY TRANSFER EQUATIONS

The Newton related method employed by Krishnamurthy and Taylor (1985a, 1985b) and Taylor and Krishna (1993) and two equation-tearing procedures, that proposed by Mori et al. (1996) and a modification introduced in this paper, will be considered in this section.

The discussion will be based on the general expression (1) and (2) for the mass transfer equations. Limiting expression, however, should be employed for large values of $| N_T/\kappa_{ij} |$ in any phase. These are presented in Appendix B of Keegan et al. (2000), along with a suggested procedure to evaluate the exponentials of $[\Psi_V]$, $[\Psi_L]$.

Newton method

The use of a Newton method is well described by Taylor and Krishna (1993). The $(3p+1)$ equations arranged in the set $\underline{F}(\underline{z}) = \underline{0}$ are the $(2p-1)$ mass transfer equation (1) and (2), the p equilibrium relations (3), the summation Eq. (4) and the heat transfer Eq. (5). The vector of unknown variables $\underline{z}$ results:

$$z^T = (N_1, N_2, \cdots, N_p, x_1^I, x_2^I, , \cdots, x_p^I, y_1^I, y_2^I, \cdots, y_p^I, T^I)$$

The following assumptions were made for the evaluations of Jacobian matrix:

- The terms $N_T(\exp[\Psi_L] - [I])^{-1}$ and $N_T(\exp[\Psi_V] - [I])^{-1}$ in the Eqs. (1) and (2) were considered to be independent of the variables in $\underline{z}$.
- Dependency of activity coefficients on temperature was ignored. ΔH_i^{vap}, h_L^* and h_V^* assumed to be constant.

The set of computer routines given by Press et al. (1994), including an step-size control modulus to induce convergence far from the solution was used to implement the Newton method.

Equation-tearing algorithm proposed by Mori et al. (1996)

The algorithm employed by Mori et al. (1996) presents two main loops. An external loop is based on the energy conservation balance, Eq. (5). Given a value of N_T, the mass transfer and equilibrium equations are solved to obtain T_I and the individual fluxes N_i. With these values and from Eq. (5) the function

$$F_I(N_T) = T_I(h_L^* + h_V^*) + \sum_{i=1}^{p} N_i \Delta H_i^{vap}(T_I) - T_L h_L^* - T_V h_V^* \quad (17)$$

can be calculated. If $F_1 = 0$, the solution has been reached. Otherwise, a new value of N_T is tried. Any root finder algorithm can be used to solve Eq. (17) on N_T. If a superlinearly convergent algorithm is used, the solution of the problem is guaranteed near the root.

The internal loop consists in solving the mass transfer and equilibrium equations, i. e. locating the point on the (T_I, N_T) curve described in previous sections, for the given value of N_T. The calculations are carried out as follows.

By equalising Eqs. (1) and (2), it is obtained

$$\underline{x}^I = \underline{x}^b + (\exp[\Psi_L] - [I])\{\underline{x}^b - \underline{y}^b - (\exp[-\Psi_V] - [I])^{-1}(\underline{y}^I - \underline{y}^b)\} \quad (18)$$

Some estimates of y_i^I, x_i^I, T_I should be defined be-

fore starting the internal loop. With these values the matrices $[\Psi_V]$ and $[\Psi_L]$ are calculated and they are left fixed while proceeding with the remaining calculations. The following sequence defines all the stages of the internal calculations:

Step 1- Provide estimates of y_i^I, x_i^I, T_I to evaluate $[\Psi_V]$ and $[\Psi_L]$.

Step 2- Calculate $x_i^I (i = 1, \cdots, p\text{-}1)$ from Eq. (18) with trial values of y_i^I (the values of y_i^I given in step 1 can be used as trial values when step 2 is performed for the first time).
Then, evaluate x_p^I from Eq. (4a)

Step 3- Evaluate y_i^I and T^I from a bubble point calculation with x_i^I values obtained in step 2.

Step 4- If the values y_i^I obtained in step 3 are approximately equal to the trial values used in step 2, step 5 is accomplished. Otherwise, another iteration starts by coming back to step 2 employing y_i^I calculated in step 3 as the new trial values.

Step 5- The individual fluxes N_i are evaluated from Eq. (2). The internal loop is finished.
The bubble point evaluation in step 3 involves an additional iterative process.
It should be note that once the internal loop has been completed, the solution does not corresponds exactly to one point on the (T_I, N_T) curve, as matrices $[\Psi_V]$ and $[\Psi_L]$ are not updated.

The loop defined by steps 2-4 can be viewed as a repeated substitution procedure with regards to variables y_i^I, i.e.

$$(\underline{y}^I)^{k+1} = \underline{G}[(\underline{y}^I)^k]$$

where k is the iteration number.
It is well known (see e.g. Burden and Douglas Faires, 1985) that such procedure is convergent only if the absolute values of the eigenvalues of the Jacobian matrix of $\underline{G}$ are smaller than the unity. By inspecting Eq. (18) it becomes clear that this condition can be fulfilled if the liquid-phase resistances to mass transfer are smaller enough than those in the vapor phase ($\underline{x}^I \approx \underline{x}^b$). Equation (18) can be rearranged to evaluate x_i^I if the opposite happens, but it can be foreseen that the procedure will fail or become unacceptably slow when mass transfer resistances in both phases are similar.

An alternative Equation-tearing procedure

To avoid the convergence weakness of Mori et al.'s algorithm, the calculations to solve the mass transfer and equilibrium equations (i.e. the internal loop) can be modified as explained below.

Instead of employing Eq. (18), the modification is based on the use of Eq. (7). Again, some estimates of y_i^I, x_i^I, T_I should be defined to evaluate matrices $[\Psi_V]$ and $[\Psi_L]$. Also, the activity coefficients necessary to evaluate K_i are calculated at the onset with those estimates and not changed in the course of the internal iterations. The following sequence defines all the stages to solve the internal calculations

Step 1- Provide estimates of y_i^I, x_i^I, T_I to evaluate $[\Psi_V]$ and $[\Psi_L]$ and activity coefficients. Calculate matrix [A] from Eq. (8).

Step 2- Evaluate K_i with a trial value of T_I.

Step 3- Calculate $y_i^I (i = 1, . . , p\text{-}1)$ from Eq. (7). Then, evaluate y_p^I from Eq. (4b).

Step 4- Evaluate x_i^I $(i = 1, . . , p)$ from the equilibrium relationships (3), employing y_i^I $(i = 1, . . , p)$ from step 3 and K_i from step 2.

Step 5- With values x_i^I from step 4 evaluate

$$F_2(T_I) = \sum_{i=1}^{p} x_i^I - 1 \qquad (19)$$

Step 6- If $F_2 \approx 0$, step 7 is accomplished. Otherwise, another value of T_I is tried and the loop is restarted from step 2.

Step 7- The individual fluxes N_i are evaluated from Eq. (2).

The assumptions made regarding $[\Psi_V]$ and $[\Psi_L]$ and activity coefficients allow function F_2 to be strictly a function of T_I. A root finder algorithm can then be used to try values of T_I required in step 6 until $F_2\ (T_I) = 0$.

Actually, the solution T_I thus found will not exactly fall on the curve (T_I, N_T) because $[\Psi_V]$, $[\Psi_L]$ and activity coefficients are evaluated from estimated values (step 1). As a consequence, Eq. (17) to be solved externally will not strictly depend on N_T, but also on the estimates used in the step 1 above. Although this fact makes the number of external iterations increase, there is in practice a considerable net saving in computations due to the simplifications made in solving the internal loop.

In short, the algorithm proposed consists of solving a nested univariate search with $F_2(T_I) = 0$ (for a given N_T) in the internal loop and $F_1(N_T) = 0$ in the external loop. Here, the same root finder algorithm is employed in both loops: a modification of the secant method based on a hyperbolic approximation to the root (Barreto and Farina, 1979), needing a couple of trial values for

initialization and showing and order of convergence 1.818.

The algorithm just described will be referred for shortness as META (modified equation-tearing algorithm). Some details concerning implementation of the META will be described below.

Solving equation (7)

The evaluation of F_2 for each internal iteration involves as major computational effort the solution of the $(p-1)$-dimensional linear system (7). This is usually performed by LU-decomposition of the matrix A followed by back-substitution. However, if for a given iteration the matrix K does not differ much from that of a previous iteration, it may be numerically convenient to solve the current system recursively, by using the available LU-decomposition of the previous matrix A. This alternative procedure is given in Appendix C of Keegan et al. (2000). It may significantly reduce computations for large numbers of components (say, $p>10$).

Estimates for step 1.

For the first entry into the internal loop, the estimates used in step 1 are those employed as the initialization values of the global algorithm, which will be discussed in the next section. At the second entry, the final values obtained as the results of the first entry are adopted. For the third entry, there are already evaluated two sets of values (y_i^I, x_i^I, T_I) corresponding to the first two tried values of N_T. Linear approximations are then used to evaluate the third set of estimates. This procedure is extended to the next entries, updating the linear approximations with the last two sets of values.

As quoted above, the employed root finder should be initialised with two trial values. One is taken as the estimate of T_I used in step 1. For the first two entries, the second value is obtained by adding one or two degrees to the estimate of T_I. Finally, for the third entry on, the value of T_I obtained in the previous entry is used as the second trial value.

Criterions to end the calculations.

The test of convergence in the internal loop is set by requiring that the difference between two successive approximations ΔT_I verifies

$$| \Delta T_I | < T_I^k e_T \tag{20}$$

where T_I^k is the last approximation to the root and e_T is the internal tolerance.

Table 6. Comparison of the behaviour of numerical procedures for four components mixtures in Fig. 2a. In all cases, $T_V=$ 335 K.

			Computing time after 10000 executions of the program (in seconds)		
h_L [W/m^2 K]	T_L[K]	κ^L; κ^V from Table	Newton	Mori et al.	META
7600	332.113	1	36	37.5	18.5
	332.113	2	29	250	24.5
	324.113	1	37	42	27.5
13000	332.113	1	43	40.6	22.0
	332.113	2	30	250	48.0
	324.113	1	37.5	53	23.5

As $N_T=0$ is a possible solution, the criterion of convergence for the external loop is established on the basis of $(\kappa_{ij}^V)_{av}$

$$| \Delta N_T | < (\kappa_{ij}^V)_{av} e_N \tag{21}$$

where ΔN_T is the difference between two successive approximations and e_N is the external tolerance.

When the internal loop is initialised with information from previous entries, as explained above, the overall precision will be established to a large extent by the external tolerance e_N. For a given value of e_N, a very small value of e_T will lead to unnecessary iterations in the internal loop. On the contrary, a very coarse value of the latter will affect the accuracy with which the external function is evaluated, increasing the number of external iterations. In general, it is expected that appropriate values of the internal tolerance should be similar to the external one.

COMPARISON OF NUMERICAL PROCEDURES

Comparison of the numerical procedures described in the last section will be made on the basis of time demanding in reaching the solution with the same degree of precision.

Tables 5-7 summarise results for the examples depicted in Figs. 1, 2a and 2b, respectively, along with the corresponding cases arisen for mass transfer coefficients defined in Table 2. Several combinations obtained with the two values of h_L discussed before and with two values of bulk liquid temperature ($T_L = T_B - 2K$) and ($T_L = T_B - 10K$) are considered.

Values for initializing the equation-tearing algorithms were $N_T = -(\kappa_{ij})_{av}$ and $N_T=0$, $\underline{x}^I = \underline{x}^b$, $\underline{y}^I = \underline{y}^b$ and $T_I = (T_B^V + T_D^L)/2$

Table 7. Comparison of the behaviour of numerical procedures for four components mixtures in Fig. 2b. In all cases, $T_V = 335$ K.

h_L [W/m^2 K]	T_L [K]	κ^L; κ^V from Table	Computing time after 10000 executions of the program (seconds) Newton	Mori et al.	META
7600	327.087	1	29.5	38	14.5
	327.087	2	23	130	17
	319.087	1	31	40.6	15
13000	327.087	1	30	38	14.5
	327.087	2	23	160	21
	319.087	1	31	44	17

Tolerances were chosen as $e_T = 10^{-3}$ and $e_N = 10^{-3}$ for the META, while the calculations were stop when the same precision was reached for the other two algorithms.

For initializing the Newton method, individual molar fluxes were set as $N_i = -(\kappa_{ij})_{av}/p$ The rest of the variables were chosen as for the equation-tearing algorithms.

For binary mass transfer coefficients given in Table 1, Mori et al.'s procedure demands systematically more time than the other two procedures. When the coefficients in Table 2 are employed, Mori et al.'s algorithm did not reach convergence or it did employing a very long computation time, reflecting the large number of iterations carried out. This behaviour is due to the fact that liquid and vapor phase coefficients in Table 2 are of the same order of magnitude, a condition for which the internal loop of Mori et al.'s algorithm is not suitable, as explained above. On the other hand, the modification proposed here for the internal loop never failed to reach convergence. Actually, the function F_2 (T_I) defined in Eq. (19) shows a monotonous behaviour for large ranges of T_I, making possible a safe convergence for each entry at the internal loop.

In general, the performances of Newton method and the META are quite similar. No trend is evident as regards possible effects introduce by the three different cases (Tables 5-7) or by the variables changed in each case (binary mass transfer coefficients, T_L, h_L): in all examples tested convergence was reached by both methods, provided that reasonable values are chosen for initializating the variables. The results in Tables 5-7 show that the META saves on average about 47% of the computing time demanded by the Newton method. This results provides evidence that substantial CPU time saving can be achieved by using the META.

Table 8. Comparison of the behaviour of numerical procedures for a water-ethanol mixture in the presence of CO_2 in a vertical shell-and-tube condenser. Operating conditions are given in Table 3.

	$T_{I(initial)}$ [K]	Computing time after 10000 executions of the program (seconds). Newton	META
Top conditions	333.8	14.5	8.45
Bottom conditions	315	12	12

The number of components in the mixture can be thought as being a factor to affect the relative performance of the methods. Nonetheless, it is difficult to predict the final effect of p as the number of elementary operations demanded by the algorithms depends on p in different ways. Solving the linear systems [sets of $(3p+1)$ equations in Newton methods and $(p-1)$ in the META] and multiplication of $(p-1)^2$ matrices (matrix exponentiation, in particular, demands several multiplications, see Appendix B of Keegan et al. (2000)) involve sets of elementary operations increasing as p^3, but another sets of operations increase as p^2 and p, in different proportions for both methods and for each problem.

To get an insight into the effect of p, all examples considered in Tables 5-7 were run again for an eight component mixture obtained by splitting each species into two fictitious isomers showing the same properties. Computing times rises by a factor of nearly four, but the ratio of times demanded by both, Newton and META, remains nearly the same (time saving becomes 43% in favour of META). These results indicate for the examples tested that the number of elementary operations required by both methods increases at nearly a second order rate with respect to p.

The performances of Newton method and META for the condensation case previously described (with conditions summarized in Table 3) have been also compared. Values for initializing the META were:

$N_T = 0.5\ N_{T,limit}$ and (as the second value) $N_T = 0$[if $F_1\ (0.5\ N_{T,limit}) < 0$] or $N_T = 0.9\ N_{T,limit}$[if $F_1\ (0.5\ N_{T,limit}) > 0$],

$y_i^I = y_i^b$, $x_i^I = \dfrac{y_i^b}{\sum_{k=1,k\neq CO_2}^{p} y_k^b}$, (for CO_2, $x_{CO_2}^I = 0$) and

T_I values are given in Table 8.

For the Newton method:

$N_i = (0.5\ N_{T,limit})/(p-1)$ (for CO_2, $N_{CO_2} = 0$), and the remaining values as for META.

The results are summarized in Table 8. Computing times of the same order are demanded by both methods, although at the top of the condenser the META performs again better.

Numerical results presented in Tables 5-8 were obtained in a PC Pentium II Processor - 350 MHz.

CONCLUSIONS AND FUTURE DIRECTIONS

Two types of numerical procedures to evaluate mass and energy transfer rates through vapor-liquid interfaces have been analysed here. Mass transfer expressions are based on Maxwell-Stefan constitutive relationships used along with the film model for both sides of the interface. The Newton method applied for the whole set of equations is compared with two equation-tearing algorithms. One of the equation-tearing algorithms is the method presented by Mori et al. (1996). The second one (META) is a modification introduced in this contribution.

Both equation-tearing algorithms involve two main loops. The internal loop consists in solving the set of mass transfer and equilibrium expressions for a trial value of the total molar flux N_T. The results are then used to check if the energy conservation equation is satisfied (external loop).

The analysis of the behaviour of mass transfer and equilibrium relationships (the equations of the internal loop referred to above) was undertaken as a first step in this study. It is found that this subset of equations can be conveniently represented by the relation between N_T and the interfacial temperature T_I (N_T, T_I curve). This relationship shows asymptotic values of T_I which can be predicted from phase equilibrium calculations and the shape of the curve depends additionally on the ratio of binary mass transfer coefficients in both phases. Maximum or minimum values of T_I may occur. A different picture arises when a non-condensable component is present in the vapor phase. In this case, a limiting total molar flux arises as T_I decreases arbitrarily. This characterisation in terms of mass and equilibrium relationships was employed to select a set of examples used afterwards to evaluate the numerical procedures. Convenient initialisation for the algorithms can also be inferred from the (known) asymptotes.

The intersection of the (N_T, T_I) curve with the energy conservation equation fixes the solution of the problem and it is what both equation-tearing algorithms actually pursue. It is shown that the problem thus formulated is well posed for reaching a numerical solution when considering real values of the mass and heat transfer coefficients and of the thermo physical properties.

The algorithm Mori et al. (1996) solves the internal loop by a repeated substitution approach. A qualitative analysis of this procedure reveals that it can not work properly when mass transfer coefficients in both phases are of the same order. It was checked numerically that the algorithm either fail to converge or it does making many iterations for cases showing such condition. The algorithm performs reasonably well, although less effectively, than the other two algorithms for the remaining cases. Since this algorithm does not involve solving linear sets of equations, it may be still a suitable alternative for some systems involving a large number of components and one of the phases being effectively mass transfer controlling.

The original purpose for introducing the META is eliminating the convergence weakness of Mori et al's algorithm. This can be readily done at the cost of adding a step requiring the solution of a set of linear equations. The algorithm showed no instance of divergence and it performed similarly for practically all examples tested. Essentially the same comments apply for Newton algorithm. A comparison of CPU time demanded by both algorithms showed better average performance by the META, saving about 50%.

On the basis of the results obtained in this contribution, the use of the META can be recommended to evaluate mass and heat transfer rates at vapor-liquid interfaces.

Future work can be concentrated in extending the analysis to a higher number of examples derived from other vapor-liquid mass exchange processes. Also, the case of multicomponent systems involving stronger liquid non-ideal behaviour than those dealt with here (e.g. close to the condition of liquid phase splitting) is of practical interest.

ACKNOWLEGEMENTS

The authors wish to thank the support of the following argentine institutions: ANPCyT (SECyT), PICT97 N° 00227; CONICET, PIP/96 N° 4791, PEI N°0524/97, UNLP, PID 11/I058.

GDM and GFB are Research Members of the Consejo Nacional de Investigaciones Cientificas y Tecnicas (CONICET). SDK has a fellowship of CONICET.

NOMENCLATURE

c_p	molar heat capacity of mixture, J/kmol K
e_T	internal loop (on temperature values) tolerance in META algorithm
e_N	external loop (on molar global flux values) tolerance in META algorithm
ΔH_i^{vap}	heat of vaporization of component i, J/kmol
K_i	phase equilibrium constant for component i
META	modified Equation-Tearing Algorithm
N_T	total molar flux , kmol/m^2 s
$N_{T,limit}$	limiting value of N_T, kmol/m^2 s
Nu	Nusselt number
N_i	molar flux of component i, kmol/m^2 s
p	number of components in the mixture
T	temperature, K
T_B	bubble point temperature, K
T_D	dew point temperature, K
x	mole fraction in liquid phase
y	mole fraction in vapor phase
h	heat transfer coefficient, W/m^2 K
h_0	global heat transfer coefficient in condensers (excludes vapor phase), W /m^2 K
$[I]$	identity matrix
P	pressure, P_a
Pr	Prandtl number
q_{latent}	latent heat flux Eq. (16), W/m^2
Sc	Schmidt number
Sh	Sherwood number

Greek letters

$[\Gamma]$	matrix of thermodynamic factors
γ_i	activity coefficient
κ_{ij}	binary mass transfer coefficient, kmol/m^2 s
$[\Psi]$	matrix of mass transfer rate factors in linearized film model

Subscripts

NC	non-condensable components
C	coolant (in condensers)
i, j	i-th, j-th components
I	the interface
L	liquid phase
V	vapor phase

Superscripts

I	the interface
b	bulk of the phase
L	liquid phase
V	vapor phase

REFERENCES

Barreto, G. F. and I. H. Farina, "An efficient method to solve systems of non-linears equations," *Chem. Eng. Sci.*, **34**, 63 (1979).

Bird, R. B. , W. E. Stewart, and E. N. Lightfoot, *Transport Phenomena*, John-Wiley and Sons, Inc., New York (1960).

Burden, R., and J. Douglas Faires, *Numerical Analysis*, PWS, Boston, USA (1985)

Henley, E. J., and J. D. Seader, *Equilibrium Stage Separation Operations in Chemical Engineering*, John-Wiley , New York, (1981).

Keegan, S. D., Mazza, G. D. and G. F. Barreto , "Appendices for Evaluation of Multicomponent Mass and Energy Transfer through Vapor-liquid Interfaces," Technical Report, Department of Chemical Engineering, National University of La Plata, Argentina (2000).

Krishnamurthy, R., and R. Taylor, "A Nonequilibrium Stage Model of Multicomponent Separation Processes. I - Model Development and Method of Solution," *AIChE J.*, **31**, 449 (1985a).

Krishnamurthy, R., and R. Taylor, "A Nonequilibrium Stage Model of Multicomponent Separation Processes. II - Comparison with Experiment," *AIChE J.*, **31**,456 (1985b).

Mazzarotta, B., and E. Sebastiani, "Process Design of Condensers for Vapor Mixtures in the Presence of non-Condensable Gases,"*Can. J. Chem. Eng.*, **73** , 456 (1995).

Mori, H., A. Oda, T. Aragaki, and Y. Kunimoto, "Packed Column Distillation Simulation with a rate-based Method," *J. Chem. Eng. Jpn.*, **29** (2), 307 (1996).

Ondry, G., I. Kim and G. Parkinson, "Reactors for the 21st Century," *Chem. Eng.* , June, 39 (1996)

Paludetto, R., G. Paret and G. Donati, "Multicomponent Distillation with Chemical Reaction Mathematical Model Analisis," *Chem. Eng. Sci.*, **47**, 2891 (1992).

Press, W. H., S. A. Teukolsky, W. T. Vetterling, and B. P. Flannery, *Numerical Recipes in FORTRAN: The Art of Scientific Computing*, Cambridge University Press, New York, USA (1994).

Sivasuvramanian, M. S., R. Taylor and R. Krishnamurthy, "A Nonequilibrium Stage Model of Multicomponent Separation Processes. IV - A novel approach to packed column design," *AIChE J.*, **33**, 325 (1987).

Taylor, R., and R. Krishna, *Multicomponent Mass Transfer*, John-Wiley and Sons, Inc., New York (1993).

Taylor, R., and A. Lucia, "Modeling and Analisis of Multicomponent Separation Processes," *AIChE Symp. Ser., USA*, **91**, 19 (1995).

(Manuscript Received February 21, 2000)